Zygote **21** (February), pp. 95–101. © Cambridge University Press 2011
doi:10.1017/S0967199411000402 First Published Online 27 July 2011

Premeiotic transformation of germ plasm-related structures during the sea urchin spermatogenesis

Arkadiy A. Reunov[1]
A.V. Zhirmunsky Institute of Marine Biology, Far East Branch of Russian Academy of Sciences, Vladivostok, Russia

Date submitted: 30.11.2010. Date accepted: 28.05.2011.

Summary

The germ plasm-related structures (GPRS) and the transformation that occurs to them during the spermatogenesis of the sea urchin *Anthocidaris crassispina* were studied by electron microscopy and morphometry. The GPRS were observed in spermatogonia and spermatocytes, but not in spermatids and sperm, which suggests an important role for these structures during the onset of meiosis. It was proposed that the germinal granules are fragmented into the compact electron-dense nuage, and fragments of the latter penetrate into the periphery of the compact electron-lucent nuage. The process of nuage integration is completed with the formation of the combined nuage, which aggregates some mitochondria into clusters. Once formed, the mitochondrial clusters undergo dissemination and assume the appearance of the dispersed nuage with mitochondrial derivatives, which in turn develops into the scattered nuage. The scattered nuage, which presumably presents the composite mixture saturated with mitochondrial matrix, terminates the GPRS transformation.

Keywords: Germ plasm-related structures, Sea urchin, Spermatogenic cells

Introduction

In various taxa of invertebrate and vertebrate animals, the spermatogonia, the cells that initiate spermatogenesis in the testes, are unique in that they have germ plasm-related structures (GPRS), such as germinal bodies (germinal granules), nuage and mitochondrial clusters (Kerr & Dixon, 1973; Satoh, 1974; Eddy, 1975; Flores & Burns, 1993; Reunov & Rice, 1993; Werner *et al.*, 1994; Reunov & Klepal, 2004; Reunov, 2006; Morroni *et al.*, 2008; Reunov *et al.*, 2009). Surprisingly, the role of GPRS is still unclear due to insufficient knowledge of both the ultrastructural and molecular mechanisms of their functioning. It should be stressed that subcellular approaches can not be applied efficiently until the morphological events have been comprehensively ascertained. Thus, a detailed investigation of GPRS by conventional electron microscopy is still needed.

[1]All correspondence to: A.A. Reunov. Department of Embryology, A.V. Zhirmunsky Institute of Marine Biology, Far Eastern Branch of Russian Academy of Sciences, 17 Paltchevsky Street, Vladivostok 600041, Russia. E-mail: arkadiy_reunov@hotmail.com

To date, one analysis of GPRS and the morphological changes that occurred during spermatogenesis in the mouse, *Mus musculus*, has been performed by Reunov (2006). This author proposed that a remarkable feature of spermatogonia was the fragmentation of the compact germinal body-like structure into nuage; these fragments bound to mitochondria, which in turn underwent membranous conglomerate detachment, which is a final stage of GPRS modification that occurs prior to meiosis. In the spermatogenesis of the sea urchin, *Anthocidaris crassispina*, the GPRS were described as that appeared as premeiotic mitochondrial clusters that were aggregated by nuage (Au *et al.*, 1998). It has also been observed that in the spermatogonia of this species, some mitochondria release their content into the cytoplasm, where these mitochondrial derivatives associate with nuage (Reunov *et al.*, 2000). However, it is not clear whether or not in this sea urchin the dissemination of mitochondria is the last stage of GPRS transformation. To address this question, it is necessary to analyse the character and order of each phase that is connected with GPRS alteration.

In this paper we describe the GPRS morphological machinery during the spermatogenesis of the sea urchin. We compared our findings with the analogous

data obtained previously for *M. musculus* (Reunov, 2006); this comparison allowed us to ascertain if mitochondrial discharge is the final step of premeiotic GPRS transformation for representatives of both invertebrates and vertebrates.

Materials and methods

Transmission electron microscopy

Sea urchins, *A. crassispina*, were collected from the subtidal region at Kat O, Hong Kong, in June 1998. In the laboratory, the gonads of three male individuals were dissected, cut into small pieces and fixed for 2 h in primary fixative (which contained 1% tannic acid and 2.5% glutaraldehyde in 0.1 M cacodylate buffer with 8.55% sucrose, pH 7.5). Fixed tissues were washed in buffer, postfixed in 2% OsO_4 for 2 h, rinsed in buffer and distilled water, dehydrated in an ethanol series and acetone, infiltrated and embedded in Spurr's resin. Ultrathin sections were stained with 2% alcoholic uranyl acetate and aqueous lead citrate before being examined on a JEOL 100 S transmission electron microscope.

GPRS count

Testes fragments from three individuals were collected. Three blocks from each individual were sectioned for transmission electron microscopy. The sections were mounted on slot grids that were coated with formvar film stabilized with carbon. One section from each block was used for counting. The ultrastructural criterions described earlier (Au *et al.*, 1998) were used for the identification of the spermatogenic cell types. A total of 20 spermatogonia, 20 zygotene/pachytene spermatocytes, 20 spermatids and 20 spermatozoa were investigated on each section. The GPRS were counted in each of 180 cells, and percentages were calculated. The results were analysed statistically using the Student's *t*-test.

Results

Spermatogonia

In the course of past and present ultrastructural observations, several types of GPRS have been observed in this category of cells. These are the germinal granules (Fig. 1*A*), the compact electron-dense nuage (Fig. 1*B*), the compact electron-lucent nuage (Fig. 1*A*,*B*), the mitochondrial clusters (see Au *et al.*, 1998; Fig. 3) and the dispersed nuage that contains mitochondrial derivatives (see Reunov *et al.*, 2000; Fig. 1*D*). The percentages of these types of GPRS were 18, 19, 22, 24 and 17% respectively (Fig. 2*A*).

The germinal granules were localized separately but tended to contact the compact electron-lucent nuage (Fig. 1*A*). The compact electron-lucent nuage was associated frequently with the cisternae of the annulate lamellae-like endoplasmic reticulum that has nuclear pore-like segments (Fig. 1*A*). Moreover, some mitochondria were frequently seen in the vicinity of both the germinal granules and the electron-lucent nuage, and some mitochondria interacted with the compact electron-lucent nuage (Fig. 1*A*).

On some sections, the compact electron-dense nuage similar to germinal granules in terms of both the ultrastructure and electron density was always registered as being in close proximity to the compact electron-lucent nuage; the mitochondria were near both types of nuage (Fig. 1*B*).

Frequently, the fragments of electron-dense nuage were observed penetrating into the periphery of the compact electron-lucent nuage (Fig. 1*C*) and were often seen distributed along the compact electron-lucent nuage surface (Fig. 1*D*). This nuage pattern, consisting of two kinds of nuage, is marked here as combined nuage. Usually, the mitochondria were seen in close contact with the combined nuage (Fig. 1*D*). As has been previously shown, the aggregates of the combined nuage serve typically as the centres for the binding of many mitochondria, giving rise to mitochondrial clusters (see Au *et al.*, 1998, Fig. 3).

Zygotene/pachytene spermatocytes

Meiotic cells of this stage were distinct from cells that are undergoing other meiotic phases by the presence of synaptonemal complexes (see Au *et al.*, 1998, in particular Fig. 6 of this paper). In these cells, the germinal granules, compact electron-dense nuage and compact electron-lucent nuage have never been found (Fig. 2*B*). The percentage of mitochondrial clusters (see Au *et al.*, 1998, Fig. 3) was about 27%, and was slightly higher than that found in spermatogonia (Fig. 2*B*). However, the percentage of the dispersed nuage that contains mitochondrial derivatives (see Reunov *et al.*, 2000; Fig. 1*D*) was much higher than in spermatogonia, at approximately 30% (Fig. 2*B*). The zygotene/pachytene spermatocytes were notable by the appearance of a new type of GPRS that could be characterised as scattered nuage, patches of which were distributed randomly throughout the cytoplasm and contained no mitochondrial derivative (data not shown). Scattered nuage are the most typical type of GPRS for zygotene/pachytene spermatocytes, making up almost 43% of the total (Fig. 2*B*).

Spermatids and spermatozoa

As has been previously shown (Au *et al.*, 1998) and is supported by the present research (Fig. 2*C*,*D*), no GPRS

https://doi.org/10.1017/S0967199411000402 Published online by Cambridge University Press

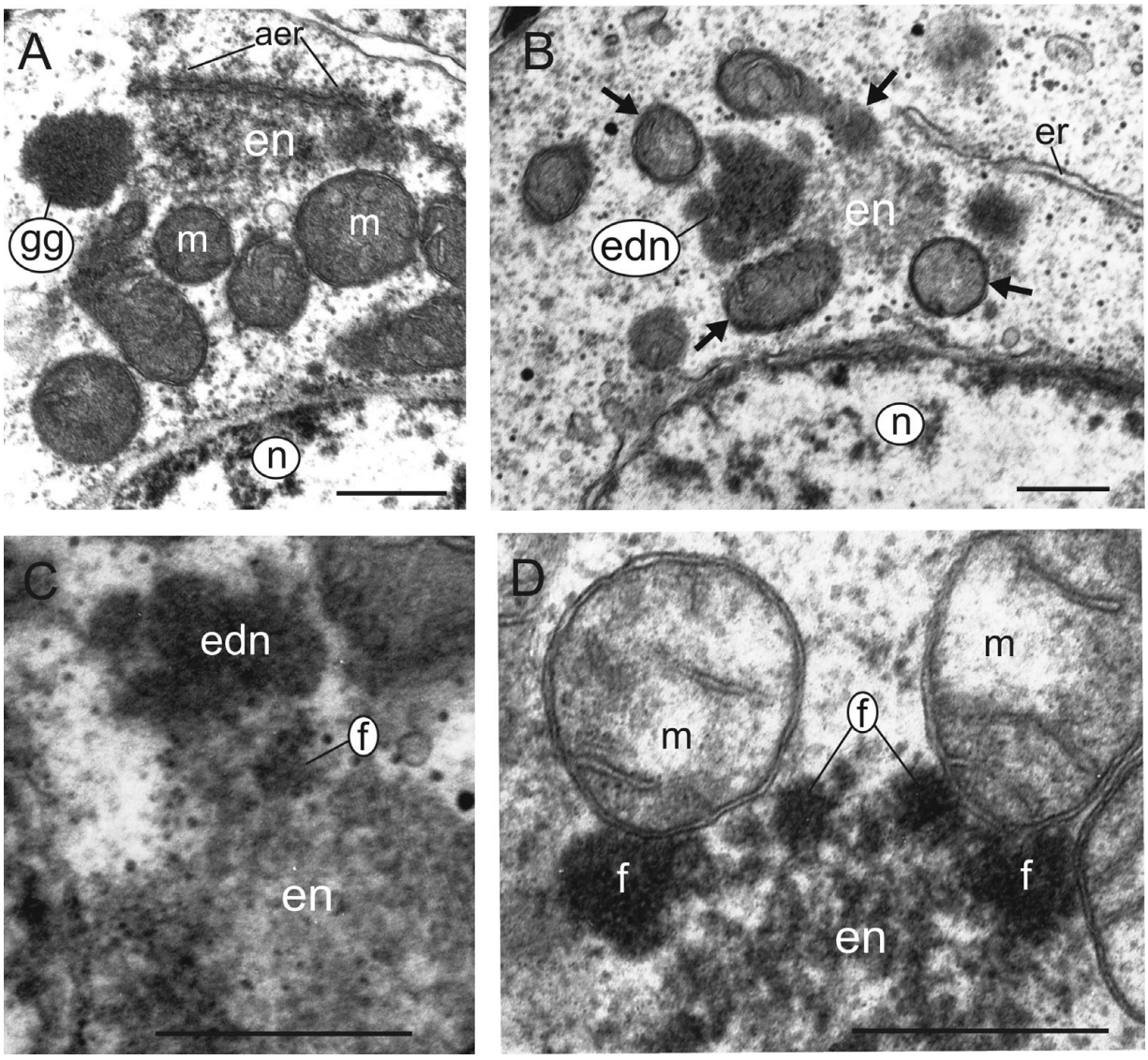

Figure 1 Transmission electron micrographs of germ plasm-related structures (GPRS) in the spermatogenic cells of the sea urchin, *Anthocidaris crassispina*. (*A*) Germinal granule (gg), compact electron-lucent nuage (en) and mitochondria (m), the structures that are located separately but tend to contact each other; note the annulate lamellae-like endoplasmic reticulum (aer) adjacent to the compact electron-lucent nuage. (*B*) Germinal granule arisen compact electron-dense nuage (edn) and compact electron-lucent nuage (en) undergoing attachment; note the mitochondria (arrows) approaching the nuage. (*C*) Germinal granule arisen compact electron-dense nuage (edn) contacting electron-lucent nuage (en); note the electron-dense nuage fragment (f) penetrating into the surface of the electron-lucent nuage. (*D*) Combined nuage consisting of electron-lucent nuage (en) and fragments of germinal granule arisen electron-dense nuage (f) located in the periphery of electron-lucent nuage; note the mitochondria (m) tightly attached to the combined nuage; n, nucleus. Bars: 0.5 μm

of any kind was found in either the spermatids or the spermatozoa.

Discussion

In the present study of *A. crassispina*, it has become clear that (in addition to the GPRS described previously such as the mitochondrial clusters, the nuage and the mitochondrial derivatives by Au *et al.* (1998) and Reunov *et al.* (2000)), the spermatogenic cells contain structures that coincide with the structural type of ribonucleoprotein bodies that are referred to as germinal granules (Chuma *et al.*, 2009). In addition, there appears to be more than one nuage category, as there are five types of nuage, such as the compact electron-dense nuage, the compact electron-lucent nuage, the combined nuage, the dispersed nuage with mitochondrial derivatives and the scattered nuage. It is remarkable that the presence of GPRS is characteristic

https://doi.org/10.1017/S0967199411000402 Published online by Cambridge University Press

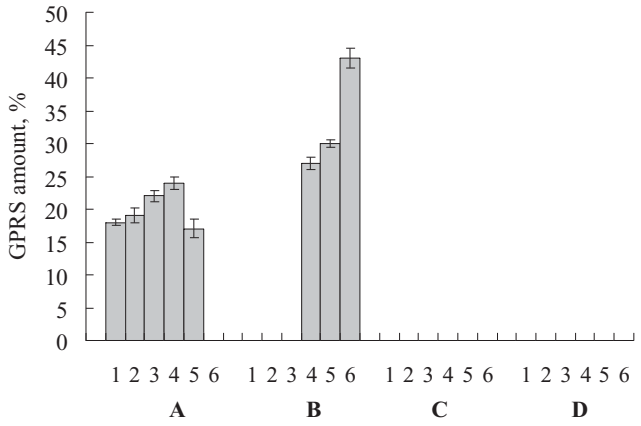

Figure 2 Diagram of the distribution of germ plasm-related structures (GPRS) in spermatogonia (*A*), zygotene/pachytene spermatocytes (*B*), spermatids (*C*) and sperm (*D*) of the sea urchin, *Anthocidaris crassispina.* 1, germinal granules; 2, compact electron-dense nuage; 3, compact electron-lucent nuage; 4, mitochondrial clusters; 5, dispersed nuage that contains mitochondrial derivatives; 6, scattered nuage.

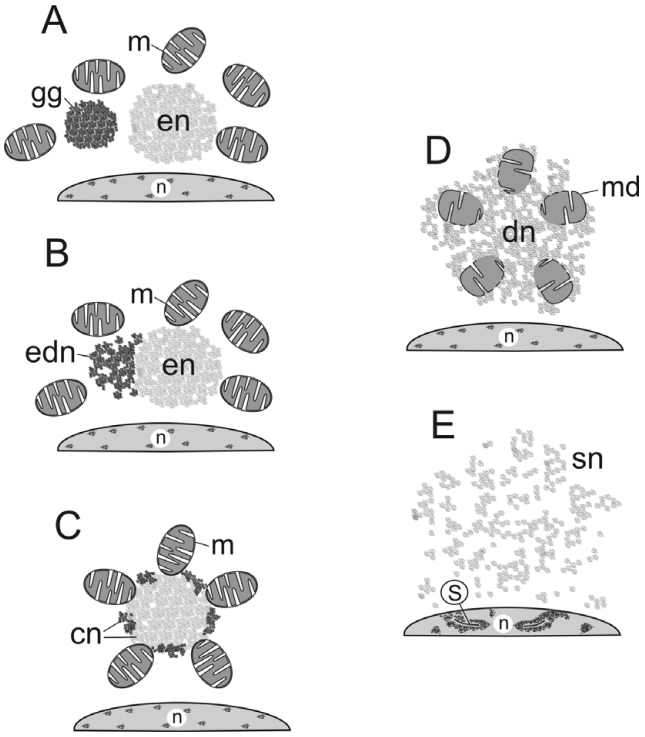

Figure 3 Schematic drawings of the germ plasm-related structures (GPRS) in the spermatogenic cells of the sea urchin, *Anthocidaris crassispina.* (*A*) Germinal granule (gg), compact electron-lucent nuage (en) and mitochondria (m) at the GPRS separate localization stage. (*B*) Germinal granule arisen compact electron-dense nuage (edn), compact electron-lucent nuage (en) and mitochondria (m) at the GPRS primary attachment stage. (*C*) Mitochondrial cluster formed by mitochondria (m) that are aggregated by combined nuage (cn) consisting of germinal granule arisen electron-dense nuage fragments (periphery) and electron-lucent nuage (center); GPRS complete attachment stage. (*D*) Dispersed nuage (dn) uptaking mitochondrial derivatives (md) at GPRS dispersion stage. (*E*) Scattered nuage (sn) at the GPRS post-dispersion stage; n, nucleus; s, synaptonemal complexes.

of only the early spermatogenic cells (spermatogonia and spermatocytes), whereas the late spermatogenic cells (spermatids and sperm) do not contain GPRS. Hence, it seems that the role of the GPRS is connected to the early phase of spermatogenesis. Therefore the next parts of the discussion are devoted to the analysis of the morphologic transformation that occurs within these structures.

GPRS in spermatogonia

It was found that the spermatogonia contained some of the GPRS types, such as the germinal granules, the compact electron-dense nuage, the compact electron-lucent nuage, the mitochondrial clusters and the dispersed nuage with mitochondrial derivatives. A better understanding of GPRS modification might be possible by tracking their morpho-spatial variants.

So far, there have been no ultrastructural data that describe if the germinal granules of *A. crassispina* are inherited or if they are formed in the spermatogonia. However, the first option seems more likely because germ plasm transfer from the late oocyte to the offspring germ cells through embryogenesis is universal for *Caenorhabditis*, *Drosophila* and *Xenopus* (Mahowald, 1977; Strome & Wood, 1982; Ikenishi, 1998). It has also been reported that germinal granule-like structures that are formed in mouse Graafian oocytes remained unchanged in the early embryos and were found in the spermatogonia (Reunov, 2004; 2006). Similar germinal granule-like structures were described in the late oocytes and embryonic cells of the holothurian, *Apostichopus japonicus* (Reunov & Alexandrova, 2006). Due to the ultrastructural similarity between *A. crassispina* germinal granules and those found in *M. musculus* and *A. japonicus*, it could be suggested that, in the sea urchin, the analogous structures are also transferred from the eggs to the offspring spermatogonia through embryogenesis. This suggestion appears quite probable, considering that the germinal granule-specific vasa RNA and VASA protein have been shown during sea urchin development by light microscopy (Juliano *et al.*, 2006; Voronina *et al.*, 2008).

Based on the similar spatial position, ultrastructure and electron density of the germinal granules and compact electron-dense nuage, it is obvious that germinal granules undergo fragmentation to compact electron-dense nuage (Fig. 3*A*,*B*). In contrast to the

https://doi.org/10.1017/S0967199411000402 Published online by Cambridge University Press

germinal granules that usually reside in the vicinity of, but not in contact with, the compact electron-lucent nuage, the compact electron-dense nuage was regularly observed closely attached to the electron-lucent nuage. This fact suggests that both structures approach each other and are then tightly co-localized (Fig. 3*A*,*B*). It seems reasonable that the morpho-spatial patterns that could be characterized here as the separate localization of the GPRS (Fig. 3*A*) and the primary attachment of the GPRS (Fig. 3*B*) assume successive phases of GPRS transformation.

The origin of electron-lucent nuage should be a subject of focused study. Because the electron-lucent nuage is attached to the endoplasmic reticulum, a finding that is strongly reminiscent of annulate lamellae (see Hodgson *et al.*, 1990; Cuoc *et al.*, 1993; Tekaya *et al.*, 1999), research is needed to determine if annulate lamellae are connected with the formation of electron-lucent nuage or if this substance has a nuclear origin, which was originally proposed for nuage (Flores & Burns, 1993; Werner *et al.*, 1994).

It should be stressed that the co-localization of different types of nuage has been reported previously in the early germinal cells of invertebrate and vertebrate representatives (Clérot, 1976; Frick & Ruppert, 1997; Klag & Ostachowska-Gasior, 1997). As has been shown by Klag & Ostachowska-Gasior (1997), the complex nuage of the primordial germ cells (PGCs) of the insect *Tetrodontophora bielanensis* arise by the aggregation of fibrous nuage that originates from the eggs and granular nuage that is extruded from the nucleus after the PGCs gonad colonization. The data of those researchers are similar to the results obtained for *A. crassispina*, in which two types of nuage form a conglomerate, characterised as the combined nuage. It appears that the nuage of multicellular animals is not simple but is instead in a compound category, the genesis of which is still understood poorly and demands further study.

In *A. crassispina*, the combined nuage results from the insertion of the compact electron-dense nuage fragments into the surface of the compact electron-lucent nuage. This combined nuage acts as the centre for binding the mitochondria and serves as the intermitochondrial cement (see Morroni *et al.*, 2008, Chuma *et al.*, 2009). It should be noted that some mitochondria are surrounded both types of nuage during two previous stages of transformation (Fig. 3*A*,*B*), and their final clustering around the combined nuage (Fig. 3*C*) seems logical. Thus, the morpho-spatial pattern of GPRS complete attachment most likely assumes that there is a third step of GPRS transformation (Fig. 3*C*).

It has been recorded that in the spermatogonia of *A. crassispina*, some mitochondria turn into mitochondrial derivatives that undergo dispersion among the spreaded nuage (Reunov *et al.*, 2000). Based on the analysis of data that has been described here, it seems possible that the alteration of the mitochondria and the spreading of the nuage may be only the result of a consistent disintegration of the mitochondrial clusters (Fig. 3*C*,*D*). The morpho-spatial pattern featured by the disintegration of the mitochondrial clusters that could be referred to as the GPRS dispersion stage could be the fourth step of GPRS transformation (Fig. 3*D*).

GPRS in zygotene/pachytene spermatocytes

The zygotene/pachytene spermatocytes were peculiar in that there was an absence of such GPRS as the germinal bodies, the compact electron-dense nuage and the compact electron-lucent nuage. This situation confirms that the function of these GPRS is completed by the zygotene/pachytene stages of meiosis. Mitochondrial clusters were present in relatively higher amounts and dispersed nuage with mitochondrial derivatives was present in significantly higher amounts, which suggests an important role for these GPRS during the zygotene and pachytene stages. Surprisingly, the scattered nuage, a substance that lacks any concrete location and that is described as particles of diffused material distributed randomly across the whole cytoplasm, was the most prevalent type of GPRS. This novel GPRS pattern may appear and proliferate exclusively as a result of the progressive disintegration of mitochondrial clusters (Fig. 3*D*,*E*). The highly prevalent morpho-spatial pattern of the scattered nuage is most likely the fifth step of GPRS transformation, characterised here as the GPRS post-dispersion stage (Fig. 3*E*). It seems possible that the scattered nuage, presumably that consists of molecules of combined nuage saturated with mitochondrial matrix, constitutes the final GPRS pattern followed by the disappearance of any GPRS during late spermatogenesis.

Mitochondrial discharge during the spermatogenesis of the sea urchin and the mouse

It became clear by comparison of the data previously obtained for *M. musculus* (Reunov, 2006) with the data from *A. crassispina* (Reunov *et al.*, 2000 and the current report) that GPRS transformation in both species have both morphological similarities as well as distinctions. Indeed, in both cases, the mitochondria are clustered by some organizing substance, but the genesis of this substance is different. In the sea urchin the substance is formed by the gradual aggregation of two components, which are the germinal granules and the electron-lucent nuage (Fig. 3*A*–*C*), but in the mouse, these clusters appear to be due to the fragmentation of one component, such as the germinal body-like structure (Fig. 4*A*–*C*). In the sea

https://doi.org/10.1017/S0967199411000402 Published online by Cambridge University Press

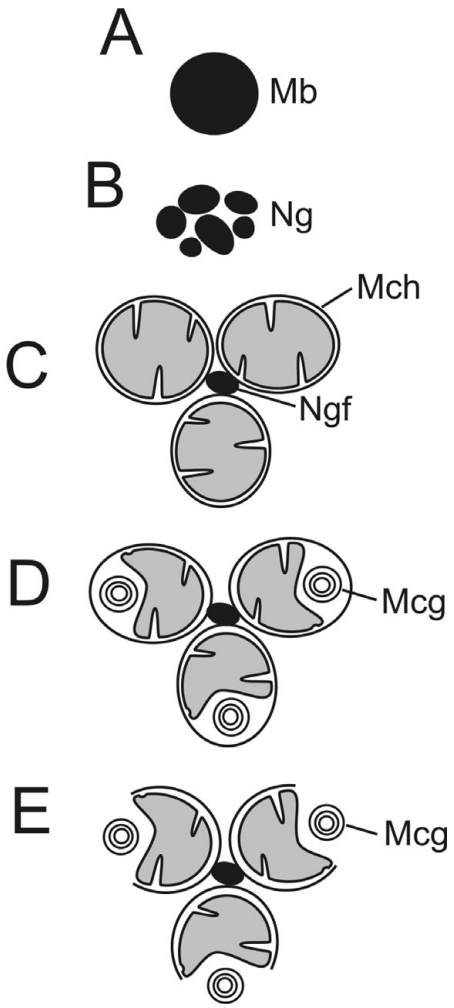

Figure 4 Schematic drawings of the germ plasm-related structures (GPRS) in the spermatogenic cells of the mouse, *Mus musculus* (from Reunov 2006). (*A*) Mitochondrion-originated germinal body-like structure. (*B*) Fragmented germinal body-like structure or nuage. (*C*) Mitochondrial cluster formed by nuage fragment. (*D*) Mitochondrial cluster with mitochondria containing membranous conglomerates. (*E*) Mitochondrial cluster with mitochondria excreting membranous conglomerates. Mb, mitochondrion-originated germinal body-like structure; Mcg, membranous conglomerate; Mch, mitochondrion; Ng, nuage; Ngf, nuage fragments (or intermitochondrial cement).

urchin, the mitochondrial clusters disappear during the gradual dissemination of the whole structural complex (Fig. 3*C*–*E*), but in the mouse, only some membranous conglomerates are released from the mitochondria that belong to the cluster (Fig. 4*D*,*E*). The release of bound mitochondria is a principally similar event that is characteristic of the premeiotic phase of spermatogenesis of both the sea urchin and the mouse despite some morphological variation. The cause of this phenomenon is still largely unknown. As the function of the membranous conglomerates that are extruded from the mitochondria still has to be investigated in the mouse, it is important to elucidate the role of the scattered nuage, enriched by mitochondrial matrix, in the sea urchin. Indeed, as has been shown by Villegas *et al.* (2002), a characteristic feature of mouse premeiotic spermatogonia is the penetration of the 16S mitochondrial RNA into the nucleus. Protein translation by the mitochondrial ribosomes has been discovered in mammalian sperm (Gur & Breitbart, 2008). It could be suggested that the mitochondrial genome plays some unexpected translational role in gamete differentiation that is accompanied by the conservation of the nuclear genome. Molecular approaches should be focused on the investigation of this role.

Acknowledgements

I am very grateful to Dr Doris Au for materials that were necessary to implement this study. This research was supported by grants from the Far East Branch of the Russian Academy of Sciences (06-III-A-06–170) and the Russian Science Support Foundation for Dr A.A. Reunov.

References

Au, D.W.T, Reunov, A.A. & Wu, R.S.S. (1998). Four lines of spermatid development and dimorphic spermatozoa in the sea urchin *Anthocidaris crassispina* (Echinodermata: Echinoidea). *Zoomorphology* **118**, 159–68.

Chuma, S., Hosokawa, M., Tanaka, T. & Nakatsuji, N. (2009). Ultrastructural characterization of spermatogenesis and its evolutionary conservation in the germline: germinal granules in mammals. *Mol. Cell. Endocrinol.* **306**, 17–23.

Clérot, J.C. (1976). Les groupements mitochondriaux des cellules germinales des poissons Téléostéens Cyprinidés. *J. Ultrastruct. Res.* **54**, 461–75.

Cuoc, C., Brunet, M., Arnaud, J. & Mazza, J. (1993). Differentiation of cytoplasmic organelles and storage of yolk during vitellogenesis in *Hemidiaptomus ingens* and *Mixodiaptomus kupelwieseri* (Copepoda, Calanoida). *J. Morphol*. **217**, 87–103.

Eddy, T.M. (1975). Germ plasm and the differentiation of the germ cell line. *Intern. Rev. Cytol.* **43**, 229–80.

Flores, J.A. & Burns, J.R. (1993). Ultrastructural study of embryonic and early adult germ cells, and their support cells, in both sexes of *Xiphophorus* (Teleostei: Poeciliidae). *Cell Tiss. Res*. **271**, 263–70.

Frick, J.E. & Ruppert, E.E. (1997). Primordial germ cells and oocytes of *Branchiostoma virginiae* (Cephalochordata, Acrania) are flagellated epithelial cells: Relationship between epithelial and primary egg polarity. *Zygote* **5**, 139–51.

Gur, Y. & Breitbart, H. (2008). Protein synthesis in sperm: dialog between mitochondria and cytoplasm. *Mol. Cell. Endocrinol.* **282**, 45–55.

Hodgson, A.N., Cross, R.H.M. & Bernard, R.T.F. (1990). *An Illustrated Introduction to the Ultrastructure of Cells*. Professional Publishers (Pty) Ltd., Butterworth, Durban.

Ikenishi, K. (1998). Germ plasm in *Caenorhabditis elegants, Drosophila and Xenopus. Dev. Growth Differ*. **40**, 1–10.

Juliano, C.E., Voronina, E., Stack, C., Aldrich, M. & Cameron, A.R. (2006). Germ line determinants are not localized early in sea urchin development, but do accumulate in the small micromere lineage. *Dev. Biol.* **300**, 406–15.

Kerr, J.B. & Dixon, K.E. (1973). An ultrastructural study of germ plasm in spermatogenesis of *Xenopus laevis*. *J. Embryol. Exp. Morphol*. **32**, 573–92.

Klag, J. & Ostachowska-Gasior, A. (1997). A cytochemical study of "nuage" accumulations in primordial germ cells of *Tetrodontophora bielanensis* (Insecta, Collembola). *Folia Biologica (Kraków)* **45**, 15–20.

Mahowald, A.P. (1977). The germ plasm of *Drosophila:* an experimental system for the analysis of determination. *Amer. Zool*. **17**, 551–63.

Morroni, M., Cangiotti, D.M., Angelo, D., Gesuita, R. & De Nectolis, M. (2008). Intermitochondrial cement (nuage) in a spermatocytic seminoma: comparison with classical seminoma and normal testis. *Virchows Arch*. **453**, 189–96.

Reunov, A.A. (2004). Is there a germ plasm in mouse oocytes? *Zygote* **12**, 329–32.

Reunov, A.A. (2006). Structures related to the germ plasm in mouse. *Zygote* **14**, 231–38.

Reunov, A.A. & Alexandrova, Y.N. (2006). The ultrastructural patterns of germinal and yolk granules in oocytes and embryonic cells of the holothurians *Apostichopus japonicus*. *Tsitologiya*. **48**, 308–14.

Reunov, A.A., & Klepal, W. (2004). Ultrastructural study of spermatogenesis in *Phoronopsis harmeri* (Lophophorata, Phoronida). *Helgolander Marine Research*, **58**, 1–10.

Reunov, A.A. & Rice, M.E. (1993). Ultrastructural observations on spermatogenesis in *Phascolion cryptum* (Sipuncula). *Trans. Am. Microsc. Soc*. **112**, 195–207.

Reunov, A.A., Isaeva, V.V., Au, D.W.T. & Wu, R.S.S. (2000). Nuage constituents arising from mitochondria: is it possible? *Dev. Growth Differ.* **42**, 139–43.

Reunov, A.A., Yurchenko, O.V., Alexandrova, Y.N. & Radashevsky, V.I. (2009). Spermatogenesis in *Boccardiella hamata* (Polychaeta: Spionidae) from the Sea of Japan: sperm formation mechanisms as characteristics for future taxonomic revision. *Acta Zoologica* **91**, 447–56.

Satoh, N. (1974). An ultrastructural study of sex differentiation in the teleost *Oryzias latipes*. *J. Embryol. Exp. Morphol*. **32**, 195–215.

Strome, S. & Wood, W.B. (1982). Immunofluorescence visualization of germ- line-specific cytoplasmic granules in embryos, larvae, and adults of *Caenorhabditis elegans*. *Proc. Natl. Acad. Sci. USA* **79**, 1558–62.

Tekaya, S., Falleni, A., Dhainaut, A., Zghal, F. & Gremigni, V. (1999). The ovary of the gonochoristic marine triclad *Sabussowia dioica:* ultrastructural and cytochemical investigations. *Micron* **30**, 71–83.

Villegas, J., Araya, P., Bustos-Obregon, E. & Burzio, L.O. (2002). Localization of the 16S mitochondrial rRNA in the nucleus of mammalian spermatogenic cells. *Mol. Hum. Reprod.* **8**, 977–83.

Voronina, E., Lopez, M., Juliano, C.E., Gustafson, E., Song, J.L., Extavour, C., George, S., Oliveri, P., McClay, D. & Wessel, G. (2008). Vasa protein expression is restricted to the small micromeres of the sea urchin, but is inducible in other lineages early in development. *Dev. Biol.* **314**, 276–86.

Werner, G., Moutairou, K. & Werner, K. (1994). Nuclear–cytoplasmic exchange during spermatogenesis of *Gryllotalpa africana* L. (Orthoptera: Gryllidae). *J. Submicrosc. Cytol. Pathol*. **26**, 219–27.